International Conference On Emerging Trends in Engineering and Management Research
NGSPM's Brahma Valley College of Engineering & Research Institute, Anjaneri, Nashik(MS) (ICETEMR-16)
23rd March 2016, www.conferenceworld.in ISBN: 978-81-932074-7-5

REGENERATIVE BRAKING SYSTEM OF ELECTRIC VEHICLE DRIVEN BY BRUSHLESS DC MOTOR

Tabish Shah[1], Dr.P.V.Thakre[2]

ME scholar[1]SSBT's COET Jalgaon, [2]Professor SSBT's COET Jalgaon

ABSTRACT

Regenerative braking can get better energy usage efficiency and can extend the driving distance of electric vehicles (EVs). A imaginative regenerative braking system (RBS) is offered in this paper. The RBS is modified to brushless dc (BLDC) motor, and it emphasize on the sharing of the braking force, as well as BLDC motor control. In this paper, BLDC motor control utilizes the conventional proportional–integral–derivative (PID) control, and the sharing of braking force adopts fuzzy logic control. As the fuzzy reasoning is slower than PID control, the braking torque can be instantaneous controlled by PID control. In an assessment to other solutions, the solution we get has better performance in regard to realization, toughness, and efficiency. Then, this paper presents the simulation results by analyzing the battery state of charge, braking force, and dc bus current under the surroundings of MATLAB and Simulink. The simulation results show that the fuzzy logic and PID control can realize the regenerative braking and can extend the driving distance of EVs under the condition of ensuring braking quality. At last, it is verified that the planned method is realizable for practical execution.

Keywords: Brushless dc (BLDC) motor, fuzzy control, proportional–integral–derivative (PID) control, regenerative braking system (RBS).

I. INTRODUCTION

IN RECENT years, electric vehicles (EVs) have received much attention as an alternative to traditional internal combustion engine (ICE) vehicles. The unprecedented focus is mainly attributable to environmental and economic concerns linked to the consumption of fossil-based oil which is used as fuel in ICE-powered vehicles. With the progress of battery and motor technology [1], the EVs become the most promising alternative to the ICE vehicles. Plug-in EVs use a battery system which can be recharged from standard power outlets. Since the performance characteristics of EVs have become comparable to, if not better than, those of traditional ICE vehicles, Evs present a realistic alternative. Regenerative braking can be used in EVs as a process for recycling the brake energy, which is impossible in the conventional internal combustion vehicles. Regenerative braking is the process of feeding energy from the

drive motor back into the battery during the braking process, when the vehicle's inertia forces the motor into generator mode.

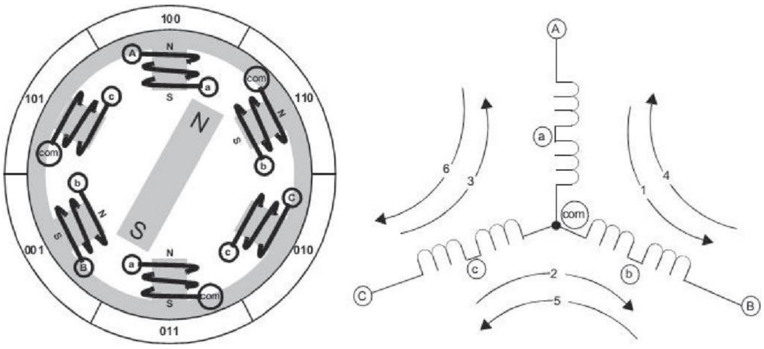

Fig. 1. Y-connected BLDC motor construction

In this mode, the battery is considered as a load, thereby providing a braking force to EVs [2]. It is shown that the use of regenerative braking of EVs can increase the driving range up to 15% with respect to EVs without the regenerative braking system (RBS). However, regenerative braking does not operate all times, e.g., when the battery is fully charged, braking needs to be effected by dissipating the energy in a resistive load. Therefore, the mechanical brake in the EV is still needed. A mechanical brake system is also

very important for EVs' safety and other operations [3]. Coordination of EV mechanical braking and regenerative braking is achieved by a single foot pedal: The first part of the foot pedal controls the regenerative braking, and the second part controls the mechanical brake. This is a seamless transition from regenerative braking to mechanical braking. It cannot be simply achieved by traditional

ICE vehicles [16].

II. MOTOR AND CONTROL

A. BLDC Motors

Brushless dc (BLDC) motors are ideally suitable for Evs because of their high power densities, good speed-torque characteristics, high efficiency, wide speed ranges, and low maintenance. BLDC motor is a type of synchronous motor. It means that the magnetic field generated by the stator and the magnetic field generated by the rotor rotation are at the same frequency. BLDC motors do not experience the "slip" which is normally seen in induction motors. However, a BLDC motor requires relatively complex electronics for control. As illustrated in Fig. 1, in a BLDC motor, permanent magnets are mounted on the rotor, with the armature windings being fixed on the stator with a laminated steel core. Rotation is initiated and maintained by sequentially energy opposite pairs of pole

windings that are said as form phases. Knowledge of rotor position is critical to sustaining the motion of the windings correctly. The information of rotor motion is obtained either from Hall effect sensors or from coil EMF measurements [4].

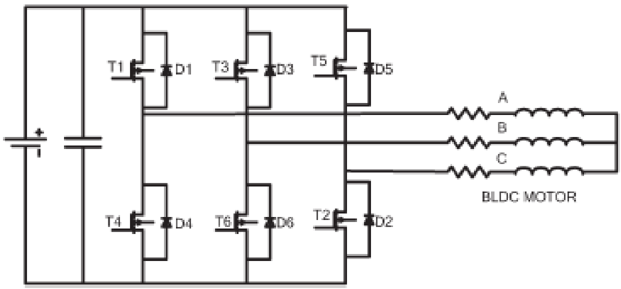

Fig. 2. H-bridge inverter circuit.

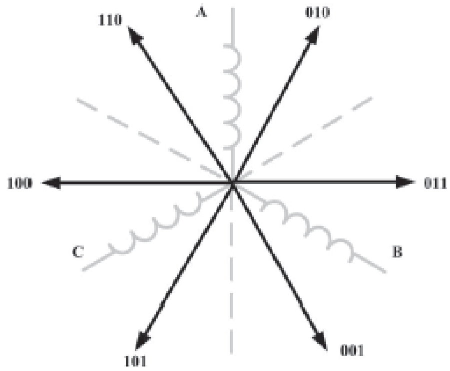

Fig. 3. Six sectors of the BLDC motor voltage vector.

B. BLDC Motor Control

BLDC motor control is the main control of the electronic commutator (inverter), and the commutation is achieved by controlling the order of conduction on the inverter bridge arm. A typical H-bridge is shown in Fig. 2. A BLDC motor uses a dc power supply which is required to provide energy. If we want to control a BLDC motor, we must know the position of the rotor which determines the commutation. Hall effect sensors are the most common sensor for predicting the rotor position. The BLDC voltage vector is divided into six sectors, which is just a one-to-one correspondence with the Hall signal six states, as illustrated in Fig. 3.

The basic drive circuit for a BLDC motor is shown in Fig. 2. Each motor lead is connected to high-side and low-side switches. The correlation between the sector and the switch states is noted by the drive circuit firing shown in Fig. 4. At

the same time, each phase winding will produce a back EMF; the back EMF of their respective windings [5] is also shown in Fig. 4. A number of switching devices can be used in the inverter circuit, but MOSFET and IGBT devices are the most

common in high-power applications due to their low output impedances [6].

C. MOSFET Control of Regenerative

Regenerative braking can be achieved by the reversal of current in the motor-battery circuit during deceleration, taking advantage of the motor acting as a generator, redirecting the current flow into the supply battery. The same power circuit in Fig. 2 can be used with an appropriate switching strategy. One simple and efficient method is to independently switch the conjunction with pulsewidth modulation (PWM) to implement an effective braking control. However, with the low speed of the BLDC motor, the winding back EMF cannot reach the voltage across the battery.Moreover, the recovery of energy also cannot be achieved. Due to the presence of inductances in motor windings, these inductances in the motor can constitute the boost circuit. In order to achieve the recovery of energy, we have to raise the voltage on the dc bus through the inductor accumulator. We turn off all MOSFET on the high arms of H-bridge and control the low arms of H-bridge with PWM. Fig. 5 shows the phase relation among the back EMF, the armature current of the BLDC motor, and the switching signals for the bidirectional dc/ac converter, in which there is only one power switch operated within each commutation state. By controlling MOSFET, the whole circuit constitutes a boost circuit. The equivalent circuit of each commutation state [7], [17] is shown in Fig. 6.

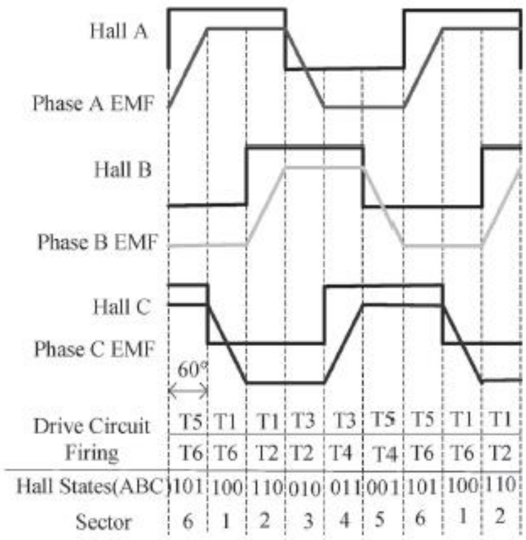

Fig. 4. Back EMF BLDC motor phase.

According to the principle of the volt-second balance, one can conclude that the net change in the equivalent inductor voltage *vL* is zero over one electric cycle, i.e.,

$$\int_{t}^{t+T_s} v_L dt = DT_s\left[2V_{\mathrm{emf}} - i_a(2R)\right] + D'T_s\left[2V_{\mathrm{emf}} - i_a(2R) - V_{\mathrm{dc}}\right] = 0 \quad (1)$$

$$i_a = 2 \cdot \frac{V_{\mathrm{emf}}}{D'^2 \cdot R_b + 2R} \quad (2)$$

where *Ts* is the switching period, *V*emf is the back EMF, and *ia* is the armature current. Similarly, according to the principle of the capacitor charge balance, one will have

$$\int_{t}^{t+T_s} i_{\mathrm{dc}} dt = DT_s\left(-\frac{V_{\mathrm{dc}}}{R_b}\right) + D'T_s\left(i_a - \frac{V_{\mathrm{dc}}}{R_b}\right) \quad (3)$$

where *D* is the duty cycle satisfying *D* + *D*_ = 1. Substituting (2) into (3), the charging voltage *V*dc can be described in terms of *D*_, the internal resistance *R* of the armature, and the equivalent load resistance *RB*, i.e.,

$$T(D') = \frac{V_{\rm dc}}{V_{\rm emf}} = 2 \cdot \frac{1}{D' + 2\frac{K}{D'}} \qquad (4)$$

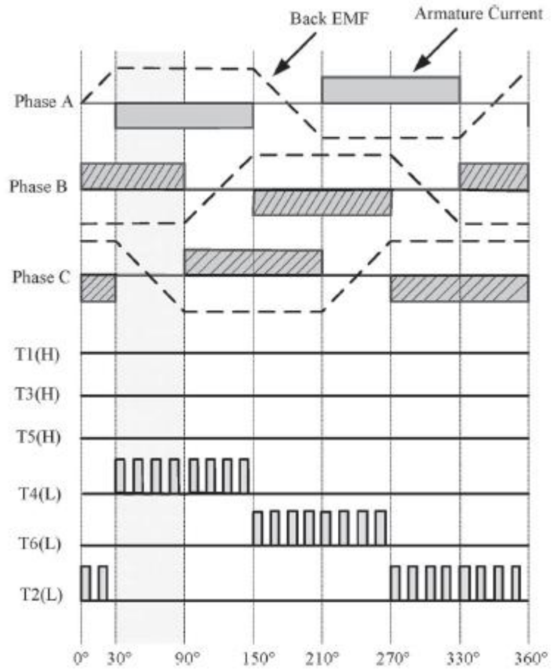

Fig. 5. Regenerative braking with single switch.

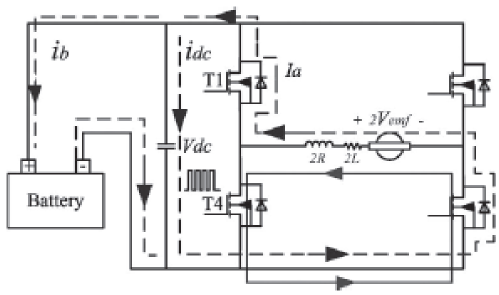

Fig. 6. Equivalent circuit of the single switch.

where *K* is defined as *R/Rb*. To evaluate the maximum conversion ratio of the switching strategy, we differentiate (4) with respect to *D_* to obtain,

$$\frac{dT}{dD'} = 2 \cdot \frac{(2K - D'^2)}{(D'^2 + 2K)^2}. \qquad (5)$$

By letting (5) be equal to 0, we can obtain the value of*D_* which maximizes (4) as follows:

$$T_{\max}(D')|_{D'=\sqrt{2K}} = 2 \cdot \frac{1}{2\sqrt{2K}} = \frac{1}{\sqrt{2K}} \qquad (6)$$

when *K* increases from 0 to l. It should be noted that the maximum conversion ratio is smaller than 1 for the case where *K* >0.5. In other words, the output voltage of the alternator commutation will be smaller than the back EMF, i.e., the dynamic energy of the EVs will be transferred into braking torque and heat instead of being recovered into the battery. Fig. 7 shows the relation.

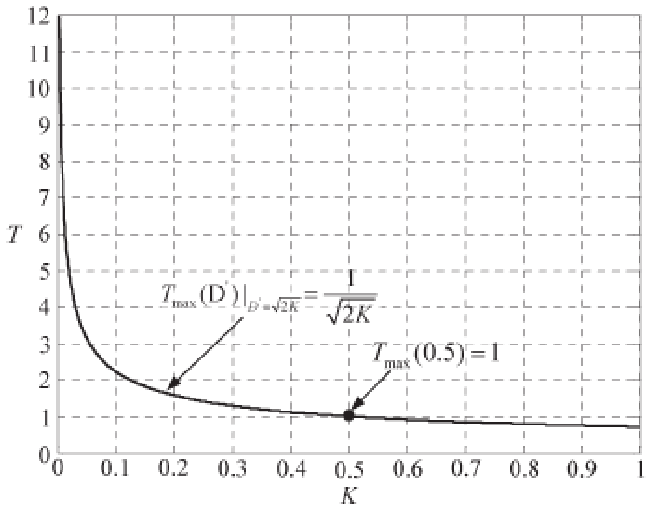

Fig. 7. Maximum conversion ratio versus *K* for regenerative braking withsingle switch.

III. EV MODELING

The modeling of the EV has been done in MATLAB/ Simulink. The driver block makes a torque request which propagates through various powertrain system component and realizes vehicle motion. System-level simulators have been modeled by using empirical data that are based on measurements supplied by component manufacturers or extended from measurements obtained from literature sources. These are modeled in Simulink as look-up tables. Other component models are physical or analytical in nature and are modeled by mathematical equations [18]. The EV model weighs about 1325 kg inclusive of battery. The vehicle has a frontal area of 2.57 m2, with a drag coefficient of 0.3 and rolling resistance of 0.00268 Ω. The values assigned are based on a rough estimate of a mid-sized car. The electric motor chosen is a BLDC motor with a peak power of 40 kW. The battery pack is a Li-Ion battery. It has a nominal voltage of 72 V, with energy content of 1.2 kWh and weight around 20 kg.

A. Driver Subsystem

The driver block delivers the desired drive torque and the desired brake torque through the activation of the accelerator and brake pedal, respectively. If the driver wishes to accelerate the vehicle, he depresses the accelerator. Depending on the amount of depression of the accelerator pedal, a corresponding driver torque request is sent to the vehicle through various powertrain systems such as the battery and motor models. The regeneration starts only when the brake pedal is pressed. Once the brake pedal is depressed, in accordance with the position of the brake pedal, a corresponding proportion of brake torque is applied. Then, the brake torque due to the regenerative brake control strategy is divided into regenerative braking and friction braking [6]. The amount of mechanical energy consumed by a vehicle when driving a prespecified driving pattern mainly depends on three factors: the aerodynamic friction losses, the rolling friction losses, and the energy dissipated in the brakes. The elementary equation that describes the longitudinal dynamics of a road vehicle has the following form:

$$m_v \frac{dv(t)}{dt} = F_t(t) - F_a(t) - F_r(t) - F_g(t) \qquad (7)$$

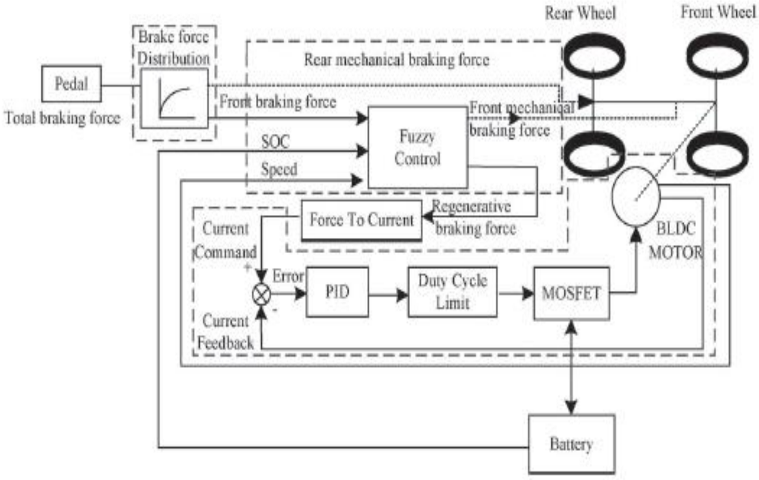

Fig. 8. Structure of the control strategy system.

where *mv* is the vehicle mass (in kilograms), *v* is the vehicle speed (in meters per square second), *Fa* is the aerodynamic friction (in newtons), *Fr* is the rolling friction (in newtons), and *Fg* is the force caused by gravity when driving on nonhorizontal roads (in newtons). The traction force *Ft* is the force generated by the prime mover minus the force which is used to accelerate the rotating parts inside the vehicle and then minus all friction losses in the powertrain.

1) **Aerodynamic Friction Losses***:*

Usually, the aerodynamic resistance force *Fa* is approximated by simplifying the vehicle to be a prismatic body with a frontal area *Af* . The force caused by the stagnation pressure is multiplied by an aerodynamic drag coefficient *Cd* to model the actual flow conditions.

$$F_a(v) = \frac{1}{2}\rho_a A_f C_d v^2. \qquad (8)$$

Here, *v* is the vehicle speed (in meters per square second), and *ρa* is the density of ambient air (in kilograms per cubic meter). The parameter *Cd* is the coefficient of drag estimated using computational fluid dynamics programs or experiments in wind tunnels. To estimate the mechanical energy, it is required to drive a typical test cycle, and this parameter may be assumed to be constant.

2) **Rolling Friction Losses***:* The rolling friction is modeled as,

$$F_r = C_r m_v g \cos(\alpha) \qquad (9)$$

where *mv* is the vehicle mass (in kilograms), *g* is the acceleration due to gravity (in meters per square second), *Cr* is the rolling friction coefficient, and *α* is the slope angle (in degrees). The rolling friction coefficient *Cr* depends on many variables. The most important influencing quantities are vehicle speed *v*, tire pressure *p*, and road surface conditions. For many applications, particularly when the vehicle speed remains moderate, the rolling friction coefficient *Cr* may be assumed to be constant.

3) **Uphill Driving Force:**

The force induced by gravity when driving on a nonhorizontal road is conservative and considerably influences the vehicle behavior. In this paper, this force will be modeled by,

$$F_g = m_v g \sin(\alpha). \qquad (10)$$

IV. SIMULATION RESULTS

Under the environment of MATLAB and Simulink, the RBS is modeled, and the drive cycle is performed. The test is performed according to urban driving schedules. The simulation results and test are represented as follows.

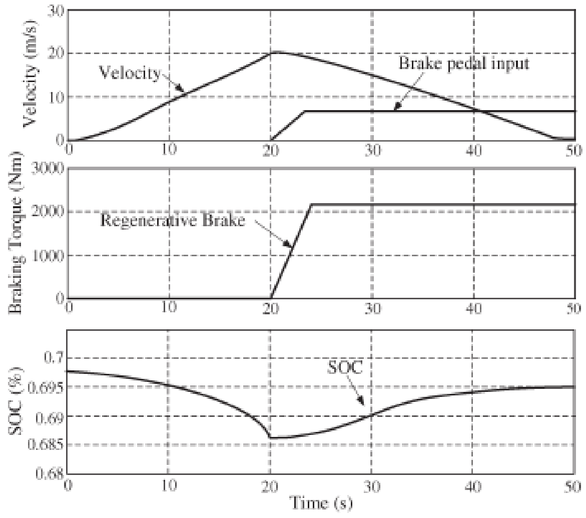

Fig. 9. Simulation EV speed curve.

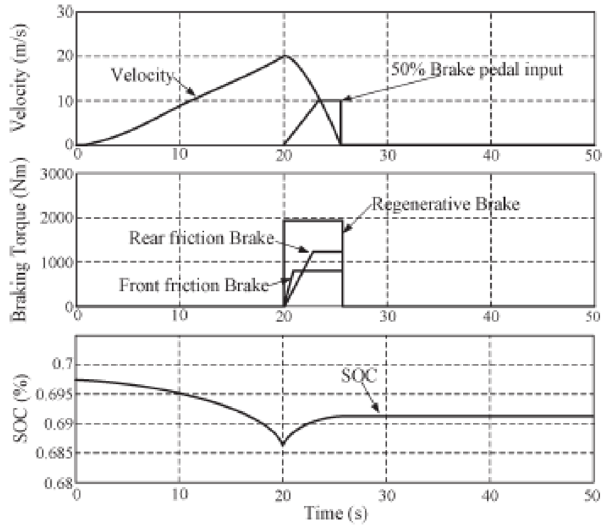

Fig. 10. Simulation EV speed curve.

V. CONCLUSION

This paper has presented the RBS of EVs which are driven by the BLDC motor. The performance of the EVs' regenerative brake system has been realized by our control scheme which has been implemented both in the simulation and in the experiments. By combining fuzzy control and PID control methods which are both sophisticated methods, RBS can distribute the mechanical braking force and electrical braking force dynamically. PID control is a very popular method in electric car control, but it is difficult to obtain a precise brake current. Braking force is affected by many influences such as SOC, speed, brake strength, and so on. In this paper, we have chosen the three most important factors: SOC, speed, and brake strength as the fuzzy control input variables. We have found that RBS can obtain appropriate brake current, which is used to produce brake torque. At the same time, we have adopted PID control to adjust the BLDC motor PWM duty to obtain the constant brake torque. PID control is faster than fuzzy control, so the two methods combined together can realize the smooth transitions. Similar results are obtained from the experimental studies. Therefore, it can be concluded that this RBS has the ability to recover energy and ensure the safety of braking in different situations.

REFERENCES

[1] P. J. Grbovic, P. Delarue, P. Le Moigne, and P. Bartholomeus, "A bidirectional three-level dc-dc converter for the ultra-capacitor applications," IEEE Trans. Ind. Electron., vol. 57, no. 10, pp. 3415–3430, Oct. 2010.

[2] F. Wang, X. Yin, H. Luo, and Y. Huang, "A series regenerative braking control strategy based on hybrid-power," in Proc. Int. Conf. CDCIEM, 2012, pp. 65–69.

[3] N. Mutoh and Y. Nakano, "Dynamics of front-and-rear-wheelindependent- drive-type electric vehicles at the time of failure," IEEE Trans. Ind. Electron., vol. 59, no. 3, pp. 1488–1499, Mar. 2012.

[4] M. Cheng, W. Hua, J. Zhang, and W. Zhao, "Overview of statorpermanent magnet brushless machines," IEEE Trans. Ind. Electron., vol. 58, no. 11, pp. 5087–5101, Nov. 2011.

[5] Y.Wang and Z. Deng, "Hybrid excitation topologies and control strategies of stator permanent magnet machines for dc power system," IEEE Trans. Ind. Electron., vol. 59, no. 12, pp. 4601–4616, Dec. 2012.

[6] C. Sheeba Joice, S. R. Paranjothi, and V. J. Senthil Kumar, "Digital control strategy for four quadrant operation of three phase BLDC motor with load variations," IEEE Trans. Ind. Informat., vol. 9, no. 2, pp. 974–982, May 2013.

[7] A. Sathyan, N. Milivojevic, Y.-J. Lee, M. Krishnamurthy, and A. Emadi, "An FPGA-based novel digital PWM control scheme for BLDC motor drives," IEEE Trans. Ind. Electron., vol. 56, no. 8, pp. 3040–3049, Aug. 2009.

[8] N. Keskar, M. Batello, A. Guerra, and A. Gorgerino, "Power Loss Estimation in BLDC Motor Drives Using iCalc," International Rectifier, El Segundo, CA, USA, Rep. AN-1048, Feb. 2010.

[9] K. Yoong, Y. H. Gan, G. D. Gan, C. K. Leong, Z. Y. Phuan, B. K. Cheah, and K. W. Chew, "Studies of regenerative braking in electric vehicle," in Proc. IEEE Conf. Sustainable Utilization Develop. Eng. Technol., Nov. 20/21, 2010, pp. 40–41.

[10] J. M. J. Yang, H. L. Jhou, B. Y. Ma, and K. K. Shyu, "A cost-effective method of electric brake with energy regeneration for electric vehicles," IEEE Trans. Ind. Electron., vol. 56, no. 6, pp. 2203–2212, Jun. 2009.

[11] N. Mutoh, "Driving and braking torque distribution methods for frontand rear-wheel-independent drive-type electric vehicles on roads with low friction coefficient," IEEE Trans. Ind. Electron., vol. 59, no. 10, pp. 3919– 3933, Oct. 2012.

[12] C.-H. Huang, W.-J. Wang, and C.-H. Chiu, "Design and implementation of fuzzy control on a two-wheel inverted pendulum," IEEE Trans. Ind. Electron., vol. 58, no. 7, pp. 2988–3001, Jul. 2011.

[13] P. J. Grbovic, P. Delarue, P. Le Moigne, and P. Bartholomeus, "The ultracapacitor based controlled electric drives with braking and ride-through capability: Overview and analysis," IEEE Trans. Ind. Electron., vol. 58, no. 3, pp. 925–936, Mar. 2011.

[14] K. Ang, G. Chong, and Y. Li, "PID control system analysis, design and technology," IEEE Trans. Control Syst. Technol., vol. 13, no. 3, pp. 559– 576, Jul. 2005.

[15] The National Standards of PR China GB/T 18386-2005, Electric Vehicles Energy Consumption and Range-Test Proceeding, China Standards Press, Beijing, China, 2005.

[16] E. Bostanci, Z. Neuschl, and R. Plikat, "No-load performance analysis of brushless dc machines with axially displaceable rotor," IEEE Trans. Ind. Electron., vol. 61, no. 4, pp. 1692–1699, Apr. 2014.

[17] Y.-T. Chen, C.-L. Chiu, Y.-R. Jhang, and Z.-H. Tang, "A driver for the single-phase brushless dc fan motor with hybrid winding structure," IEEE Trans. Ind. Electron., vol. 60, no. 10, pp. 4369–4375, Oct. 2013.

[18] A. Dadashnialehi, A. Bab-Hadiashar, Z. Cao, and A. Kapoor, "Intelligent sensorless ABS for in-wheel electric vehicles," IEEE Trans. Ind. Electron., vol. 61, no. 4, pp. 1957–1969, Apr. 2014.